Evidence of anomalous losses of fusion products on JET

Yu.Baranov[1] , I.Jenkins[1], V.Kiptily[1], J.Ongena[2], V.Yavorskij[3,4] and JET EFDA contributors*
JET-EFDA, Culham Science Centre, Abingdon OX14 3DB, UK
[1] *Euratom/CCFE Fusion Association, Culham Science Centre, Abingdon OX14 3DB, UK*
[2] *LPP-ERM/KMS, Association Euratom-'Belgian State', TEC Partner, Brussels, Belgium*
[3] *Association EURATOM-OEAW, Institute for Theoretical Physics, University of Innsbruck, Austria*
[4]*Institute for Nuclear Research, Ukrainian Academy of Science, Kiev, Ukraine*

Abstract

Fast ion losses in tokamak plasmas are considered to be neo-classical in many applications. Recent fast ion loss measurements of the fusion products on JET have provided information on the loss mechanism of the fusion products. A simulation of the JET fast-ion loss detector data demonstrates that fast fusion tritons and protons may experience super-banana diffusion significantly exceeding the neoclassical level.

Experimental data and its simulation

Losses of the fast ions have been measured in a wide range of optimised shear and standard H-mode plasmas on JET. The scintillator probe (SP) [1] allows the detection of lost ions at a single position outside the plasma. It is located just below the mid-plane of the torus. The probe detects energetic ions (E>250keV). The main source of such ions in pulses without ICRH is a fusion reaction D+D→p(3.0MeV)+T(1.0MeV). The design of the camera allows measuring losses as a function of their pitch angle θ and Larmor radius ρ, shown in Figure 1a by the horizontal and vertical grid lines, respectively. The spread of the loss footprint in the vertical direction is defined, mainly, by the detector response function and by the width of the distribution function of the tritons/protons in energy.

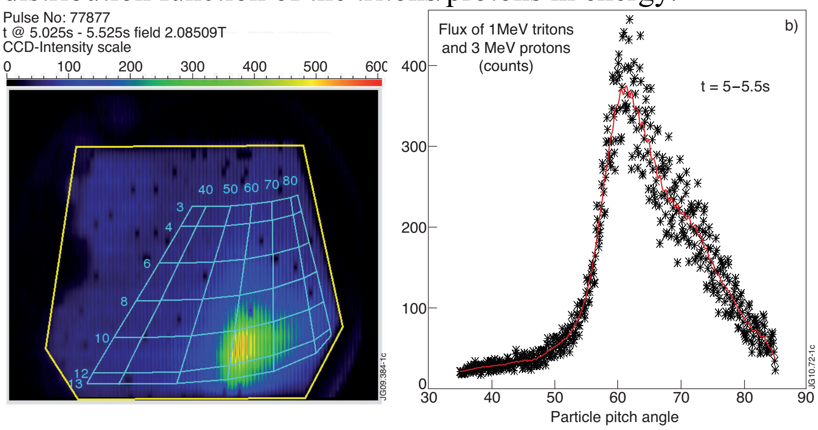

Figure 1. Pulse #77877. Signal integrated over 5-5.5s. a) Image of the lost fast tritons/protons born in the plasma and passing through the SP window. The vertical lines of the grid show the Larmor radius and the horizontal lines show the pitch angles. b) Loss profile at the fixed Larmor radius ~11.4cm (triton energy ~ 0.9MeV, proton energy ~ 2.7MeV)

The horizontal spread of the losses can be interpreted by analysis of the trajectories of the fusion products born in different parts of the plasma cross section. Modelling of the triton and proton orbits shows that the region of the SP with highest brightness, $\rho=\rho_m$, $\theta=\theta_m$, corresponds to the trajectories of trapped particles passing in the vicinity of the magnetic axis. Particles with trajectories crossing the equatorial plane at the high or low magnetic field sides strike the scintillator at $\theta< \theta_m$ or $\theta> \theta_m$, respectively. A pitch-angle loss profile at the fixed Larmor radius $\rho = \rho_m$ is shown in Fig.1b. It provides a measured dependence of the lost tritons/protons on the pitch angle $F_m(\theta, \rho = \rho_m)$ at the location of the scintillator probe. It is worth noting that the distribution function of the tritons at their birth is practically isotropic. Taking into account all these facts, we can conclude that $F_m(\theta, \rho = \rho_m)$ provides information on the radial distribution of the birth rate of the fusion products and their loss rate.

The SP response function depends on several design features. The angle α between the detector window surface and the magnetic field reduces the flux of the particles with pitch angle θ by a factor of $\sin(\theta+\alpha)/\sin(\theta)$. The probe window is covered by a 1μm gold foil. This foil induces a pitch angle scattering, which could be approximated by a combination of two Gaussian functions with width $\sigma_T(\beta)= 0.87\exp(-(\beta/4.75)^2)+0.13\exp(-(\beta/10)^2)$ for 1MeV tritons and $\sigma_p(\beta)=0.86\exp(-(\beta/1.55)^2)+0.14\exp(-(\beta/3)^2)$ for 3MeV protons, where β is the scattering angle in degrees. Equal fluxes of 2-3MeV protons and 0.7-1MeV tritons induce 44% and 56% of the measured light, respectively. The mapping of the pitch angle and Larmor radius on the SP camera image introduces an additional correction factor, which depends on the local magnetic field and α. The ion energy should be corrected with respect to SP "measured" Larmor radius/energy due to 10% energy loss in the gold foil in the probe window.

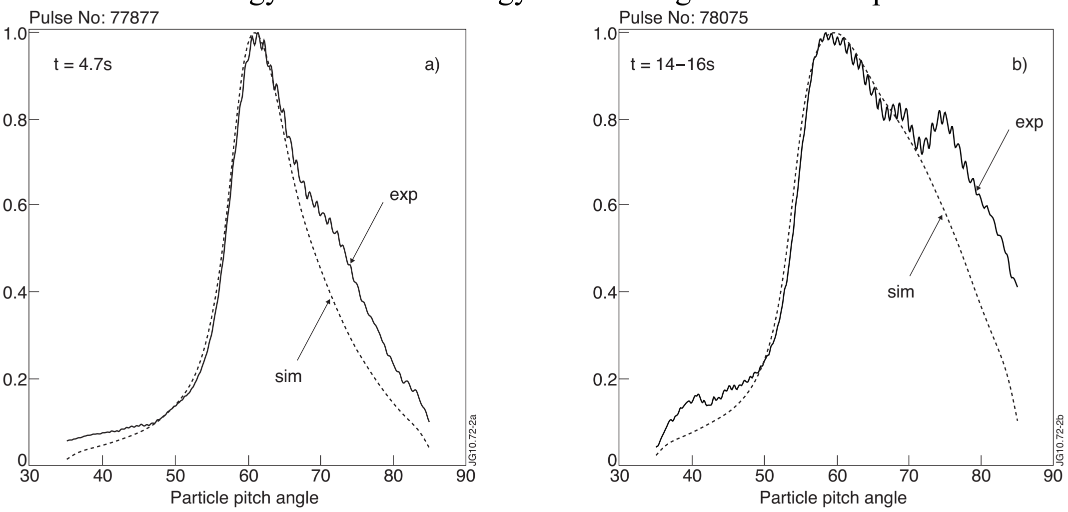

Figure2. a) 1.75 MA / 2.7 T, H-mode, 20MW NBI, $n_{eped}=4.10^{19}m^{-3}$, q(0)=1.7, q_{95}=4.6, elon=1.73, triang=0.37, c) 2.5 MA / 2.6 T, H-mode, 20MW NBI, $n_{eped}=4.8\ 10^{19}m^{-3}$, q(0)=1.0, q_{95}=3.6 elon=1.67 triang=0.27

The distribution function of the lost fusion products $F_s(\theta, \rho = \rho_m)$ was simulated by TRANSP [2] and corrected with the detector response function. It should be noted that the triton distribution function in TRANSP at birth is a delta function in energy space $\delta(E-E_{oT})$, where energy $E_{oT} \approx$1MeV. The proton distribution function is assumed to be equal to the triton distribution $\delta(E-E_{op})$ with E_{op}=3MeV. The exact details of the fusion product trajectories depend on the plasma equilibrium. Its accurate description was verified by reproducing the MSE measured q-profiles.

Results of the modelling assuming the neoclassical fast ion behaviour were compared for a number of optimised shear and standard H-mode discharges without ICRH and strong fishbone modes, which may affect the SP signal. The distribution functions $F_s(\theta)$ and $F_m(\theta)$ are shown in Fig.2 for two typical cases in the normalised form as the SP is not absolutely calibrated. The modelled $F_s(\theta)$ reproduce measured $F_m(\theta)$ reasonably well in the central part of the pitch angle range $50^o \leq \theta \leq 70^o$. Fusion products with such pitch angles registered by the

SP come predominantly from the plasma core. This suggests that the source of the fusion products in the core and their losses are in agreement with neoclassical theory. However, a sensitivity of the calculated $F_s(\theta)$ is weak to moderate anomalous diffusion of the beam ions D_{an}<1m^2/s in the plasma core (r/a<0.3) and it can not be ruled out. There is a discrepancy

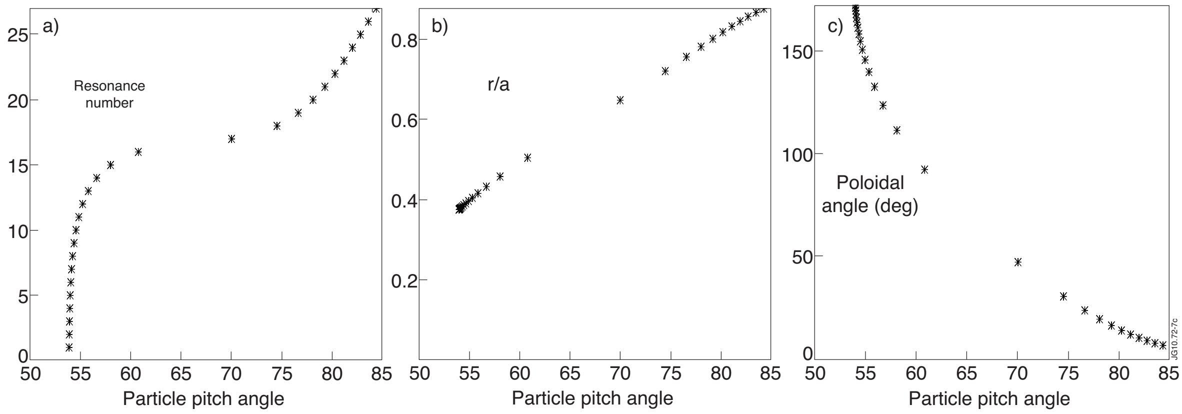

Figure 3. a Resonance $32\omega_p$-$L\omega_b$=0 number vs. pitch angle θ at the plasma boundary. b) Radial location of banana tip for resonance ions, c) Poloidal location of the banana tip for resonance particle. Calculated in circular geometry for 1 MeV tritons. Pulse #78075, t=15s.

between $F_s(\theta)$ and $F_m(\theta)$ in the region of large $\theta \geq 70^o$. It is believed to be associated with a super-banana diffusion of trapped fusion products [3,4]. It occurs when there is a resonance $N\omega_p - L\omega_b = 0$ between the toroidal precession frequency ω_p and bounce frequency ω_b of the trapped ions, where N is a number of toroidal coils and $L = 0, \pm 1, \pm 2, ..$. The spatial distribution of such resonances is shown in Fig.3 for one of the pulses from Fig.2. A calculation of the resonance condition has been done for circular plasma cross section. Modelling of selected trajectories in real geometry and equilibrium [5] is in qualitative agreement with results of Fig.3, although it gives slightly smaller resonance L numbers. This is confirmed by Fig. 4 where marginally confined drift

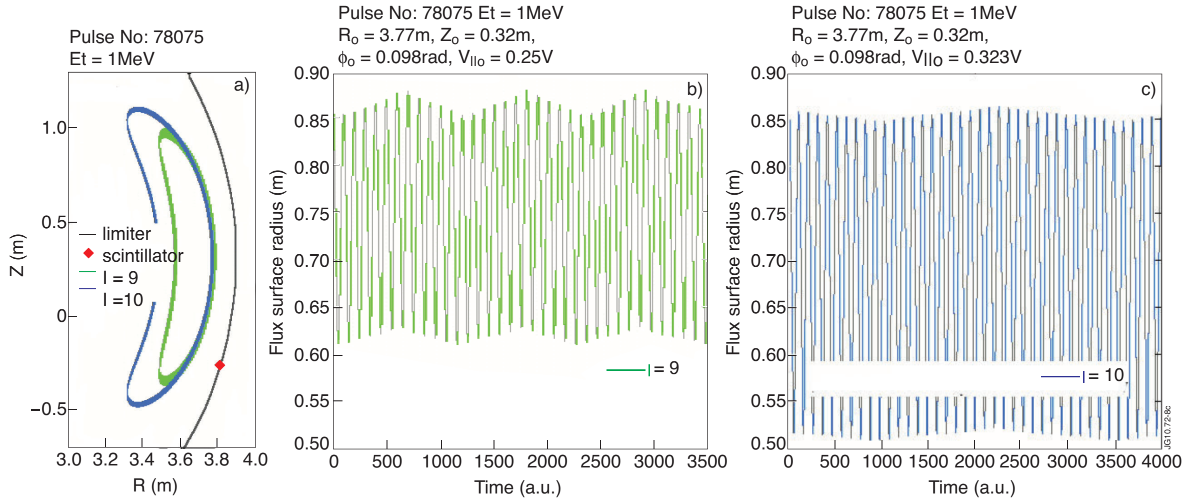

Figure 4. a) L=9 and L=10 super-banana orbits of 1MeV tritons in shot 78075; b, c) super-banana oscillations of the radial coordinate of the guiding centre for orbits shown in figure a).

super-banana orbits of 1MeV tritons with L=9 and L=10 are shown. It should be noted that locations of banana tips and the L numbers for resonance particles depend strongly on the q-profile. Notably the highest resonance numbers L are concentrated in the peripheral region

(0.5<r/a<1) and small poloidal angles. The ripple amplitude δ in this region increases significantly as can be seen in Fig.5a. The abundance of the resonances in the narrow range of large pitch angles and their closeness creates a favourable condition for enhanced super-banana diffusion of the resonant particles. This type of diffusion increases significantly above the neoclassical level in the region where $\delta > \delta_1 = \varepsilon / (Nq)^{3/2}$ in the regime of low collisionality. Such regime is fulfilled in area where $\omega_{sb} \cong \left(V\rho_L / (Rr)\right)(\delta/\delta_1 + \sqrt{\delta/\delta_1}) > \nu_{eff} = \nu_{\perp}((Nq)^2/\varepsilon)(1+\sqrt{\delta_1/\delta})^2$ [4] as shown in Fig.5b. Collisionless stochastic diffusion is realised when δ>δ_{GWB} [6], where $\delta_{GWB} = (\varepsilon / Nq)^{3/2} / (\rho_L dq/dr)$. Estimated diffusion coefficient for 1MeV fusion tritons [4] $D = ((r/Nq)/(1+\sqrt{\delta_1/\delta}))^2 \nu_{eff} / (1+(\nu_{eff}/\omega_{sb})^2)$ is shown in Fig.5c. The diffusion coefficient significantly increases at the plasma periphery.

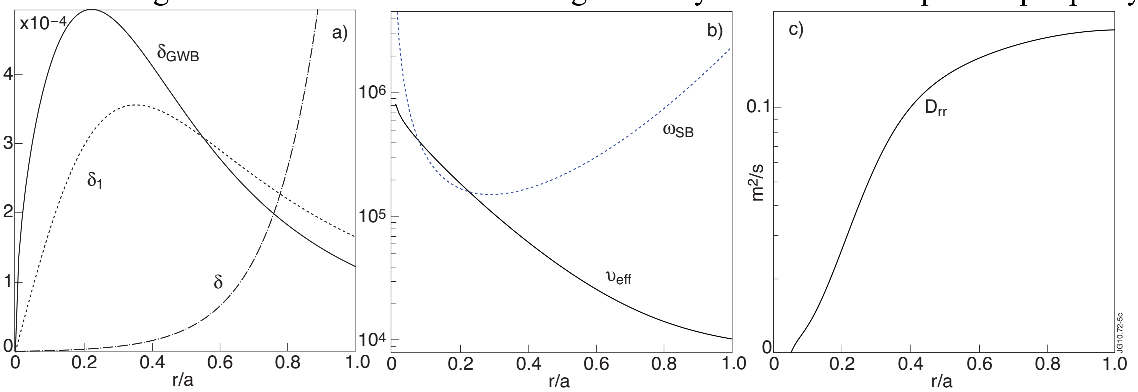

Figure 5. a) Approximated standard JET ripple amplitude δ in the equatorial plane, Goldston White Boozer ripple amplitude threshold δ_{GWB} [6] and critical ripple amplitude for collisional super-banana fast ion losses δ_1. b) super-banana precession frequency and effective collisional frequency [5]. Estimate of effective diffusion coefficient. Pulse #78075, t=15s

In conclusion, SP probe measurements and modelling of the fast fusion product losses demonstrated that their source is well described in the region of r/a<0.5 in the absence of ICRH and strong Fishbone MHD activity assuming the neoclassical diffusion of the beam ions. The fusion ions in the outer region of the plasma r/a>05 with pitch angles θ>70 may experience anomalous diffusion. The localisation, energy and pitch angle of the lost particles are consistent with the super-banana diffusion in the limit of small collisions. This type of diffusion may significantly exceed the level of neoclassical diffusion.

This work was carried out within the framework of the European Fusion Development Agreement and was partly funded by the United Kingdom Engineering and Physical Sciences Research Council under grant EP/G003955 and by the European Communities under the contract of Association between EURATOM and CCFE. The views and opinions expressed herein do not necessarily reflect those of the European Commission.

* See the Appendix of F Romanelli et al., Fusion Energy (Proc. in 22nd IAEA Fusion Energy Conference, Geneva, 2008) IAEA (2008)

References

[1] Darrow D.S et al. Rev.Sci.Instrum. 75 (2004) 3566
[2] Goldston, R.J., et al J.Comput.Phys. 43 (1981) 61
[3] Mimata, H. et al. Plasma Fusion Res. 4 (2009) 008
[4] Yavorskij V.A. et al. Phys.Plasmas 6 (1999) 3853
[5] Yavorskij V.A. et al. EPS 2006, paper P1.066.
[6] Goldston R.J et al. Phys.Rev.Lett. 47(1981) 647